

2 **Advances in crest factor minimization for wide bandwidth**  
3 **multi-sine signals with non-flat amplitude spectra<sup>†</sup>**4 **Helena Althoff<sup>1</sup>, Maximilian Eberhardt<sup>1</sup>, Steffen Geinitz<sup>1\*</sup> and Christian Linder<sup>1</sup>**5  
6 <sup>1</sup> Fraunhofer Institute for Casting, Composite and Processing Technology (IGCV);

7 email: info@igcv.fraunhofer.de

8 \* Correspondence: steffen.geinitz@igcv.fraunhofer.de; Tel.: +49 821 90678 222

9 † Presented at the 1st Online Conference on Algorithms, 27/09/2021 - 10/10/2021.

10 **Abstract:** Multi-sine excitation signals give spectroscopic insight in fast chemical processes over  
11 bandwidths from 10<sup>1</sup> Hz to 10<sup>7</sup> Hz. The crest factor (CF) determines the information density of a  
12 multi-sine signal. Minimizing the CF yields higher information density and is the goal of the pre-  
13 sented work. Four algorithms and a combination of two of them will be presented. The first two  
14 algorithms implement different iterative optimizations of the amplitude and phase angle values of  
15 the signal. The combined algorithm alternates between the first and second optimization algorithm.  
16 Additionally, a simulated annealing approach and a genetic algorithm optimizing the CF were im-  
17 plemented.18 **Keywords:** multi-sine signals, crest factor, crest factor optimization, iterative optimization, dielec-  
19 tric analysis, simulated annealing, genetic algorithms20 **1. Introduction**21 Dielectric analysis (DEA) is a well-known method for characterization of material  
22 behavior and a technology for monitoring chemical processes, e.g. the curing thermoset-  
23 ting resins [1], the curing of adhesives [2] or the polymerization process of polyamide 6  
24 [3]. A more general term is electrical impedance spectroscopy (EIS) [4]. In the context of  
25 biological processes it is also referred to as bio-impedance spectroscopy (BIS) [5].26 Independent of the application, DEA compares the phase and amplitude of a sinus-  
27 oid excitation signal applied to a sensor in contact with a specimen with its response sig-  
28 nal. Changes in phase and amplitude over time give indication about the state of the spec-  
29 imen. Ongoing chemical reactions creating new molecular structures result in changing  
30 dielectric behavior which can further be used to correlate other physical parameters or  
31 states, e.g. the viscosity or the state of cure.32 Apart from being a characterization method, DEA has the benefit of being applicable  
33 for process monitoring and process control [6, 7]. Therefore, showing great potential for  
34 inline quality monitoring solutions for adhesive part assembly or 3D printing using fast  
35 curing resins [8].36 Historically, in order to achieve full spectroscopic results sweeping approaches using  
37 single frequency sine waves were used. Especially for fast processes that take place in a  
38 few seconds or less, new approaches are needed to achieve spectroscopic information.  
39 Multi-sine signals provided the means to achieve the desired results. Nevertheless, using  
40 multi-sine excitation signals with only few frequencies for process monitoring and relying  
41 on absolute values limits the usage in industrial applications drastically, as the measure-  
42 ment principle is prone to disturbances from external influences, e.g. contamination or  
43 parasitic induction. Further, the use of only a small number of frequencies limits the in-  
44 formation necessary to derive a complete picture of the processes or effects occurring –  
45 not only in the time domain but also in the frequency domain.27  
28 **Citation:** Lastname, F.; Lastname, F. 28  
29 Lastname, F. Title. *Proceedings* 2021, 29  
30 68, x. <https://doi.org/10.3390/xxxxx> 3031  
32 Published: 27.09.2021 3233 **Publisher's Note:** MDPI stays neu- 33  
34 tral with regard to jurisdictional 34  
35 claims in published maps and institu- 35  
36 tional affiliations. 3640 **Copyright:** © 2021 by the author 40  
41 Submitted for possible open access 41  
42 publication under the terms and 42  
43 conditions of the Creative Commons 43  
44 Attribution (CC BY) license 44  
45 ([http://creativecommons.org/licenses](http://creativecommons.org/licenses/by/4.0/)  
46 /by/4.0/).

In [8, 3] an approach is shown using multi-sine excitation signals with up to 20 frequencies incorporated giving spectroscopic insight in fast chemical processes for high bandwidths. With recent modifications, the system is now able to monitor a bandwidth from  $10^2$  Hz to  $10^7$  Hz resulting in a need for excitation signals with more than 20 frequencies distributed over the measurement bandwidth to provide sufficient spectral resolution.

To compare the generated signals objectively metrics are needed which give insight in the signals and the information they contain. One commonly used metric is the crest factor (CF). The CF determines the information density of a multi-sine signal. Minimizing the CF yields higher information density and is the goal of the presented work.

### 1.1. Multi-sine

Large bandwidth impedance spectroscopy (IS) requires a dedicated/specific excitation signal. The main requirement towards these signals is that they allow for a combined analysis of the signals in the time and frequency domain. Multiple options have been reported for these applications in literature over the past decades. The most commonly used signals are binary sequences as maximum length binary sequences (MLBS) [9] or discrete interval binary sequences (DIBS) [10], chirp signals [11] and multi-sine signal signals [12]. Multi-sine signals for large bandwidth impedance analysis offer several advantages over other signal types. They allow for a custom amplitude spectrum while having customizable excitation frequencies.

The signal is generated by adding up multiple sine waves, while each wave can be chosen with its particular frequency  $f_n$ , amplitude  $a_n$  and phase  $\varphi_n$  according to the following equation:

$$u(t) = \sum_{n=1}^N a_n \cos(2\pi f_n t + \varphi_n). \tag{1}$$

### 1.2. Crest Factor

A widely used metric to evaluate and compare multi-sine signals in the time domain is the use of the crest factor (CF). This metric shows how much amplitude is consumed by a signal to introduce a certain amount of energy into a system [13]. Higher values indicate harmonics, while low values for multi-sine imply no or little interferences between the specific frequencies. The CF is calculated as the ratio between the peak value of a signal and its effective (root mean square) value:

$$CF = \frac{U_{peak}}{U_{RMS}}. \tag{2}$$

For a signal in the time domain  $s(t)$  measured over a time interval  $[0; T]$  the CF is calculated according to the following formula:

$$CF(s) = \frac{\max_{t \in [0, T]} |s(t)|}{\sqrt{\frac{1}{T} \int_0^T |s(t)|^2 dt}}. \tag{3}$$

## 2. State of the Art

Current methods used for optimization of multi-sine signals are either analytical approaches for calculating the phase angles or iterative algorithms. The idea behind the analytical formulas is to control the crest-factor (CF) by choosing the phases of the regarded components of the multi-sine appropriately. One of the first attempts to solve this problem has been proposed by Schroeder [14]. His approach adapts the phase angles of the single multi-sine components according to the following formula:

$$\varphi_m = \varphi_0 - 2\pi \sum_{n=0}^{m-1} (m-n) \frac{|a_m|^2}{\sum_{k=0}^{M-1} |a_k|^2}, \tag{4}$$

with  $a_i$  being the amplitude of the  $i$ -th component,  $m = 1, \dots, M - 1$  and  $\varphi_0 \in [-\pi, \pi]$ . Schroeders approach was adopted by Newman [15] yielding a slightly different formula for optimal phase angles:

$$\varphi_n = \frac{\pi n^2}{N}, n = 0, 1, \dots, N - 1. \tag{5}$$

A major difference between these two formulas is, that Schroeder took the amplitude values of the different frequency-components of the multi-sinesignal into account, whereas Newmans method only uses the number of exciting frequencies. Therefore, Schroeders scheme often gets better results in case of non-constant amplitudes [13].

By now further approaches to solve this problem analytically have been presented. In recent years several formulas have been introduced by Ojarand [16]. These three equations  $\Phi_i^1, \Phi_i^2, \Phi_i^3$  calculate the phase angle for frequency component  $i$ . They are quite easy to calculate and behave well especially for sparse frequency distributions. In the first case the formula also shows promising results for denser frequency distributions:

$$\Phi_i^1 = Bi^2, \Phi_i^2 = 180 \frac{B}{i}, \Phi_i^3 = 180 \frac{B}{\sqrt{i}} \tag{6}$$

The parameter  $B$  can be freely chosen inbetween 0 and 180 and  $i$  stands for the currently regarded frequency component. The five formulas described above all behave different from another depending on the distribution of the frequencies. Nonetheless it must be pointed out, that these methods do not achieve acceptable results in terms of the CF.

Using iterative algorithms to optimize the phase angles values promises to be a more satisfying approach. Several versions of well-behaving algorithms have been presented in the last decades and yet they do not yield optimal solutions. These can so far only be provided by an exhaustive search of all possible phase combinations. Within the last few years Ojarand proposed two different iterative algorithms [16, 17].

The first one, which has been presented in 2014, optimizes the phase angles by selectively searching through a given range of phase angles. Hence, this algorithm takes a lot of time to find suitable phases for each frequency. For 20 or more frequency components it would takes days to optimize their phase angle, which makes this algorithm unsuitable for industrial applications.

In 2017 Ojarand et al. presented another algorithm trying to solve existing problems with their algorithms only finding local minima. This is a well-known problem that appears with iterative algorithms that minimize the CF of multisine signals [17]. Therefore, the main idea of their new method was to start the iteration with a fixed phase set, calculated by an analytical formula. After that, the multisine signal is modulated. Then the main part of the algorithm starts, consisting of another iteration in which they first build the Fourier spectra and calculate the inverse discrete fourier transformation (IDFT). Thereafter the CF of the resulting signals needs to be calculated and compared to the currently lowest CF. In case of an improvement of the CF, the currently optimal phase set gets updated. Subsequently they use a logarithmic clipping function to clip the current multisine signal and then calculate the discrete fourier transformation (DFT) for this signal. The last step is needed to obtain a new phase set from the DFT that may yield a lower CF. This iteration can be executed an arbitrary number of times. At the end, a new phase set is calculated by one of the analytic formulas and then the whole process described above is being repeated.

As mentioned before, the first algorithm achieves quite low CFs, because it selectively searches the whole given phase spectrum for a near to optimal phase angle

combination. This comes at the cost of taking more and more time for an increased number of frequencies in the multisine signal. Therefore, this algorithm is not useful for the application discussed in this paper. The second algorithm on the other hand returns promising results, especially for signals whose frequencies are distributed over a rather small bandwidth.

### 3. Optimization approaches

In the following three new iterative algorithms that minimize the CF will be presented and subsequently tested to compare their performance in terms of CF minimization to the algorithm Ojarand presented in 2017.

#### 3.1. Iterative-stochastic Optimization

The first new algorithm comprises two separate components, an iteratively operating algorithm and a stochastic algorithm. The iteratively working algorithm optimizes the CF of the currently regarded multisine by optimizing the phase angles.

An overview over the workflow of the algorithm is given in Figure 3 (Appendix). The algorithm starts with calculating a first set of phases, e.g. the formulas (6). In our implementation we use the formula  $\Phi_i^2(k) = 180 B/i$ . Then, each phase angle is being regarded and optimized separately. To achieve this, every phase angle once gets in- and once decreased. The multi-sine signal is modulated using the new phase angle resulting in a new multi-sine differing in only one component. At the end of this iteration the CF of the new signal can be calculated and compared to the previous one to update the so far best-found phase set. Summing up, this iteratively working algorithm searches for a minimum that is located close to the consigned set of phases. Therefore this algorithm only delivers a local optimum and should be used in combination with other globally acting algorithms.

To handle the drawback of the first introduced algorithm, a second one has been developed to combine it with. This second one operates stochastically. The idea behind this algorithm is to calculate random phase angles  $\varphi$  and amplitude values  $a_i$  in a specified range. For the  $i$ -th component they are defined as follows:

$$W_\varphi = [0, 2\pi], W_{a_i} = [0.9A_i, 1.1A_i] \quad (7)$$

where  $A_i$  is the amplitude value of the  $i$ -th component that has been calculated at the beginning of the algorithm.

We restrict the amplitudes because the originally prescribed distribution of the amplitudes should keep its form preferably. As a result, the newly calculated amplitude value may deviate by a maximum of 10% from the value calculated at the beginning. This stochastic algorithm alternately calculates a set of random phases angles and then random amplitude values. These are then used to modulate a new multisine signal and compare its CF to the lowest CF reached so far. In case of an improvement it saves the better phase respectively amplitude values and continues the random calculations.

To combine the benefits of both above described algorithms, the iterative-stochastic optimization algorithm alternates between the iterative and the stochastic algorithm. That way the chance of finding the global minimum rises and the chance of getting stuck in a local minimum is minimized. The algorithm terminates when a set number of CF calculations is reached.

#### 3.2. Simulated Annealing

In addition, a Simulated Annealing (SA) approach is adapted for the specified problem. SA is a metaheuristic to approximate a global optimum. The algorithm consists of iteratively executed steps. For each problem, the components of annealing schedule, acceptance probability  $p$ , current state  $s$ , state transition and cost function have to be defined. [18]

The annealing schedule reduces the start temperature  $T_0$  at each iteration  $k$  until it reaches the final Temperature  $T_f$  and the algorithm terminates. We used a schedule where the current temperature  $T_k$  is reduced at each iteration  $k$  by the cooling factor  $c$  according to:

$$T_k = T_{k-1} * c \tag{8}$$

Furthermore, the algorithm keeps track of the current state that corresponds to a possible solution for the problem. Each state consists of a phase angle and amplitude value for each frequency component. At the start, the state of both parameters is randomly initialized. Afterwards, a neighbor state is selected at each iteration by changing a phase angle or amplitude value of a randomly chosen frequency-component according to the value range of equation (7).

The current state  $s_{k-1}$  transitions into the neighbor state  $s_k$  if the crest factor (CF) of the neighbor state is smaller than the current state. It also transitions into the neighbor state with the acceptance probability:

$$p_k = e^{-\frac{CF(s_k)-CF(s_{k-1})}{T_k}} \tag{9}$$

Otherwise, the current state is kept. At the end, the algorithm returns the state with the lowest CF. The specific configuration of the algorithm is based on several test runs and consists of the parameter:  $T_0 = 100$ ,  $T_f = 0.00005$  and  $c = \left(\frac{T_f}{T_0}\right)^{\frac{1}{n_{CF}}}$ , where  $n_{CF}$  specifies the number of CF calculations. The parameter  $n_{CF}$  can be chosen freely and determines the runtime duration.

### 3.3. Genetic Algorithm

The genetic algorithm (GA) is another metaheuristic that we adopted for the specified problem. GA is part of the domain of evolutionary algorithms and is defined by the components: initialization, selection, crossover and mutation [19].

At the beginning, multiple candidate solutions are randomly generated to build a start population. Each of these is characterized by chromosomes that model the properties of a solution. A chromosome, in turn, is modeled as the phase angle and amplitude value of a frequency component. Afterwards, the iterative process begins with the selection of parents for the next generation.

We use tournament selection for the selection process. The tournament size  $k$  is set to the value of 3 and each candidate is chosen randomly. The best candidate of the tournament is selected based on the lowest CF. Then a crossover operation generates the offspring by combining two selected individuals. For that matter, a uniform crossover that chooses random chromosomes from either parent with equal probability is used.

A mutation operation at the end of the iteration changes for each offspring the amplitude and phase angle of each frequency component with probability:

$$p_{mut} = \frac{1}{2 * n_{freq}}, \tag{10}$$

where  $n_{freq}$  specifies the number of frequency components. The mutation changes a phase angle or amplitude value by randomly choosing a new value in the specified value ranges of these parameters mentioned in equation (7).

These steps are repeated until the final number of generations  $n_{generation}$  is reached. To compare our approaches, we use the number of CF calculations  $n_{CF}$  to specify the runtime duration. Therefore, we set:

$$n_{generation} = \frac{n_{CF}}{n_{pop}}, \tag{11}$$

where  $n_{pop}$  is the population size. We set the population size equal to 100 and the probability for keeping the original parent in the next population to 40 %. The specified configuration was determined by trial-and-error.

### 3.4. Experiments

According to the intended application scenarios, different parameters were selected for a detailed investigation. Three amplitude distributions – uniform, linear, exponential (both latter decreasing with increasing frequency) – are of importance for our research. The upper bandwidth was limited to  $10^6$  Hz as this was a reasonable tradeoff between CF reduction and calculation effort. The frequency distribution was fixed as was the number of iterations.

All possible combinations from Table 1 are tested for each algorithm. A random start state is used which is the same for all algorithms. Furthermore, each configuration gets executed five times due stochastic events. An exception is the algorithm from Ojarand as it always delivers the same result.

**Table 1.** Experiment configuration.

Parameter	Value
Frequency bandwidth	$10^2 - 10^6$
Number of frequencies	10, 20, 50, 100
Frequency distribution	Linear
Amplitude distribution	Uniform, Linear, Exponential
$n_{CF}^1$	40,000

<sup>1</sup> Number of CF calculations.

To conduct the experiments the calculations were executed on Microsoft Azure using the programming language Python. The used hardware configuration was a Standard-F32s-v2 compute unit using 32 virtual Intel(R) Xeon(R) Platinum 8272CL CPUs with 2.60GHz. The memory size as well as the Storage (SSD) was set to 64 GiB. A separate process with an individual configuration is started on each CPU Core in parallel.

## 4. Results and Discussion

### 4.1. CF minimization

The results for the specified configurations and algorithms are visualized in Figure 1. Each Figure represents the results for a specific amplitude distribution. The abbreviation Mixed stands for iterative-stochastic optimization algorithm and Clip for the algorithm presented from Ojarand [16]. Furthermore, Schroeders analytic formula from equation (4) is used as a baseline. Using stochastic elements SA, GA and Mixed were calculated several times. Thus, showing the mean and standard deviation of the CF after  $n_{CF}$  iterations.

All presented algorithms outperform Ojarand’s algorithm and Schroeder’s formula in terms of CF. SA in general delivers the best results, followed by GA and iterative-stochastic algorithm. Especially for multi-sine with large numbers in frequencies the outperformance becomes significant large with up to one to one and a half in CF.

In summary, a broad range of algorithms is compared on predefined conditions. The advantage is that comparability between different algorithms on uniform conditions is created. Nevertheless, a limited selection of algorithms and hyperparameter optimization was done. Therefore, it is not guaranteed that there are more suitable algorithms for the specified problem. Furthermore, the presented algorithms do not always deliver the same results. We tried to analyse this effect by running the algorithms multiple times, but five repetitions are not enough to give a general statement. Nevertheless, our tests indicate only small deviations between different runs.

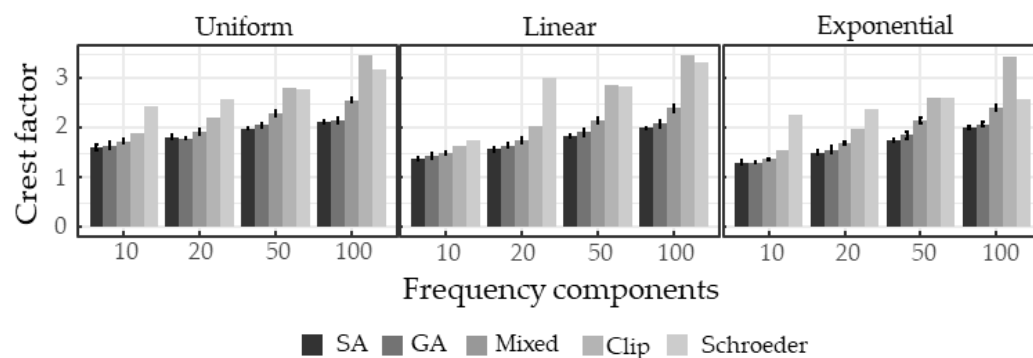


Figure 1. CF Results for all runs.

4.2. Time per CF reduction

The runtime and progression of the algorithms is analyzed by investing the improvement of the CF over time. Figure 2 illustrates this process. Hereby, the improvement  $\Delta CF$  is calculated by taking the difference between the best-found CF until a specific iteration and the start value. Only the results for 50 frequency components are shown due to limited space. Nevertheless, the CF progression for the other frequency components is similar. For each iteration the mean and standard deviation over all five repetitions of an algorithm is calculated and visualized with one exception. Due to the lack of stochastic events, the Clip algorithm is not calculated multiple times. The actual runtime can be calculated by taking the time taken for each iteration from Table 2.

The results show that the final CF for Clip and Schroeder is surpassed by all presented algorithms after only a few iterations. Schroeder’s formula results lie around the final CF of the Clip algorithm. See Figure 1 for comparison. The high reduction lasts until iteration 10,000. Afterwards, it slows down. One exception is SA because it depends on the predefined annealing schedule. Therefore, the characteristic curve is always the same regardless of the number of iterations. Nevertheless, the curve of SA shows that the start phase where the algorithm is purely random and the last phase seem very long. This is an indication that a more diligent hyperparameter search could accelerate the algorithm.

Furthermore, none of the algorithms are optimized for runtime and the values from Table 2 are only reference values. These runtime values depend strongly on various parameters, such as hardware configuration, programming language or parallelization. Another topic is the standard deviation of different runs compared between the algorithms. In general, the deviation is not as pronounced in the SA algorithm as in the iterative-stochastic and GA method.

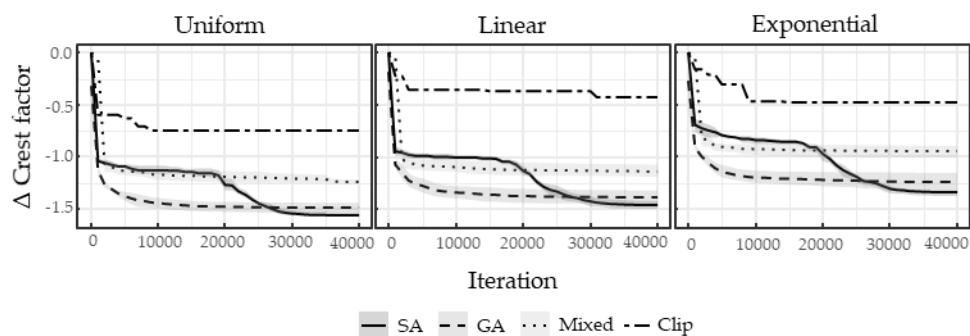


Figure 2. Progression for 50 frequency components.

**Table 2.** Time per Iteration in seconds.

Configuration		Time per Iteration [sec]			
Frequency components	Amplitude distribution	SA	GA	Mixed	Clip
10	Uniform	0.328	0.328	0.322	0.923
10	Linear	0.327	0.329	0.321	0.919
10	Exponential	0.326	0.328	0.321	0.922
20	Uniform	0.560	0.572	0.560	1.145
20	Linear	0.559	0.567	0.533	1.151
20	Exponential	0.560	0.566	0.530	1.148
50	Uniform	1.081	0.959	1.034	1.704
50	Linear	0.978	0.855	0.900	1.576
50	Exponential	0.790	0.717	0.646	1.350
100	Uniform	1.967	2.002	1.980	2.404
100	Linear	1.967	2.000	1.979	2.406
100	Exponential	1.058	1.054	1.059	1.093

### 5. Conclusions and future work

Using multi-sine signals with low CF is a necessity for high precision measurement systems as the DEA relying on the comparison of excitation and response signals. Due to non-linearities in the electrical components as well as disturbances in the measuring path a signal with low CF is favorable as the frequency analysis becomes more robust. Thus, resulting in a less prone measurement device.

With an increase in bandwidth, an increase in frequencies monitored is required. Especially if the analysis is difficult to support by a model-based approach using small sets of measurement points for the model fit. For industrial applications, where environmental influences, contamination, material aging, differences between material batches are more rule than exception a fast implementation is required and a simplified approach is preferred. The presented methods have shown significant improvements for reaching low CF as well as obtaining fair CF in a short amount of time especially for high numbers of frequencies over a wide bandwidth. Thus, the foundation was laid to apply analytical methods based on the evaluation of the time depended frequency behavior over a wide bandwidth that will open up new paths for the investigation of fast curing adhesives or similar chemical processes and phase changes in thermoplastic.

Our plans for future research are to investigate the effect of different start values e.g. Schroeder’s or Newman’s formula on the performance and results of our presented algorithms. These formulas do yield considerably better results than random values for the phase angles and could therefore have a significant impact. Further improvement of our presented algorithms will also be a topic. For the iterative-stochastic method, a selective search instead of the current iterative search is a timesaving option. In addition, the runtime needs to be inspected more. For example, the algorithms can improve by using a more runtime-oriented programming language or parallelization. Another issue is to ensure reliability of the algorithms by increasing the amount of repetitions.

**Author Contributions:** “Conceptualization, S. Geinitz and M. Eberhardt; methodology, S. Geinitz, M. Eberhardt, C. Linder; software, M. Eberhardt, H. Althoff, C. Linder; validation, H. Althoff and C. Linder; formal analysis, H. Althoff, C. Linder; writing—original draft preparation, M. Eberhardt, C. Linder, H. Althoff and S. Geinitz; writing—review and editing, M. Eberhardt, C. Linder, H. Althoff and S. Geinitz.; visualization, C. Linder and H. Althoff; supervision, S. Geinitz; project administration, S. Geinitz; funding acquisition, S. Geinitz. All authors have read and agreed to the published version of the manuscript.”

1                                   **Funding:** “This research was funded by the Administration of Swabia and the Bavarian Ministry of  
2                                   Economic Affairs and Media, Energy and Technology.”

3                                   **Informed Consent Statement:** “Not applicable”

4                                   **Conflicts of Interest:**

5                                   “The authors declare no conflict of interest.”

6                                   “The funders had no role in the design of the study; in the collection, analyses, or interpretation of  
7                                   data; in the writing of the manuscript, or in the decision to publish the results”.

8

Appendix

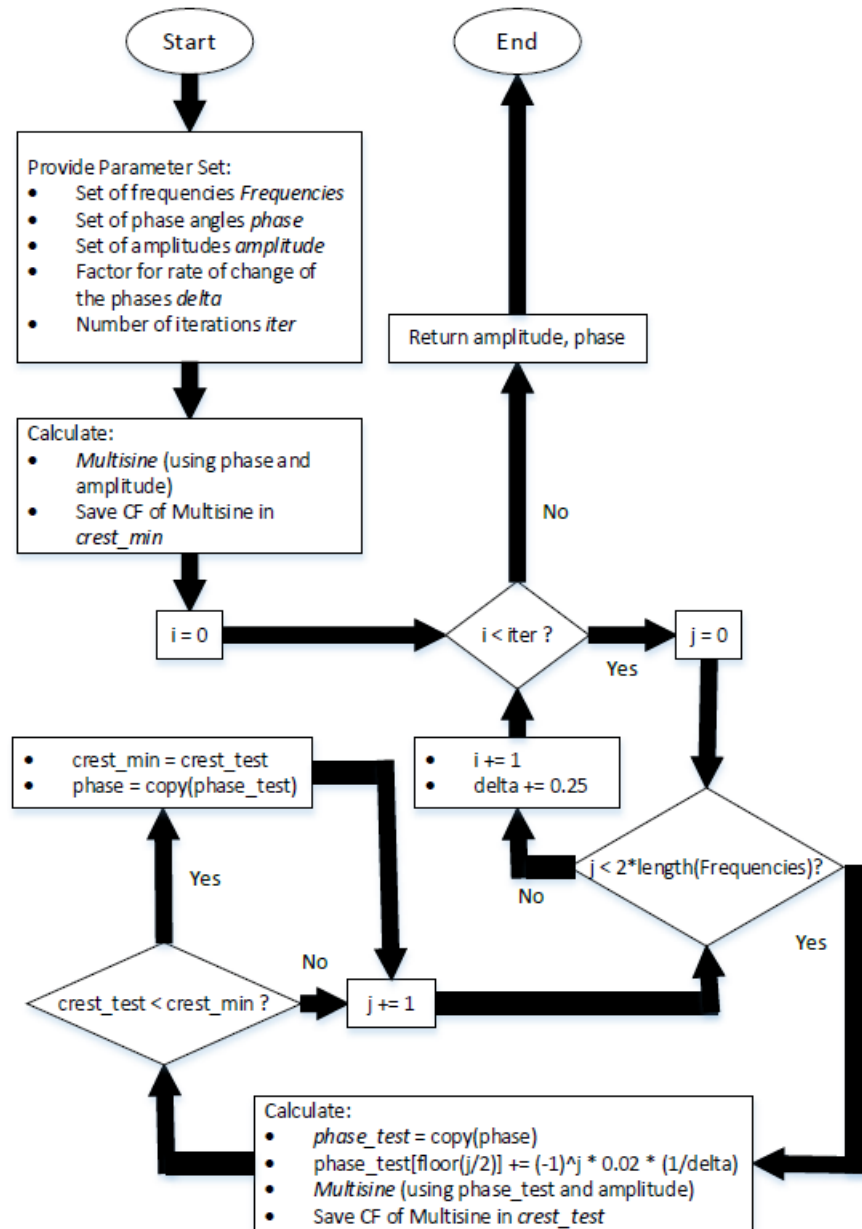


Figure 3. Iterative optimization algorithm.

References

1. F. Martin, A. Koutsomitopoulou, I. Partridge, A. Skordos, Dielectric Cure Monitoring of a Fast Curing Resin System, 2015.
2. L. H. Garden, D. Hayward, R. A. Pethrick, Dielectric non-destructive testing approach to cure monitoring of adhesives and composites. *Proceedings of the Institution of Mechanical Engineers, Part G: Journal of Aerospace Engineering* 2007, Vol. 221, Issue 4, pp. 521–533.

- 1 3. M. Eberhardt, S. Geinitz, R. Wendel, F. Henning, K. Drechsler, Simultaneous Multi-Frequency Dielectric Analysis of the  
2 Polymerization Process of Anionic Polyamide 6, in: *Proceedings of the 2019 International Conference on Composite Materials*  
3 (RMIT University 2019), pp. 2873–2884.
- 4 4. D. D. Stupin, E. A. Kuzina, A. A. Abelit, A. K. Emelyanov, D. M. Nikolaev, M. N. Ryazantsev, S. V. Koniakhin, M. V.  
5 Dubina, Bioimpedance Spectroscopy: Basics and Applications. *ACS Biomaterials Science & Engineering* 2021, Vol. 7, Issue 6,  
6 pp. 1962–1986.
- 7 5. V. Sirtoli, K. Morcelles, J. Gómez, P. Bertemes-Filho, Design and Evaluation of an Electrical Bioimpedance Device Based on  
8 DIBS for Myography during Isotonic Exercises. *Journal of Low Power Electronics and Applications* 2018, Vol. 8, p. 50.
- 9 6. D. E. Kranbuehl, P. Kingsley, S. Hart, G. Hasko, B. Dexter, A. C. Loos, In situ sensor monitoring and intelligent control of  
10 the resin transfer molding process. *Polym Compos (Polymer Composites)* 1994, Vol. 15, Issue 4, pp. 299–305.
- 11 7. A. McIlhagger, D. Brown, B. Hill, The development of a dielectric system for the on-line cure monitoring of the resin transfer  
12 moulding process. *Composites Part A: Applied Science and Manufacturing* 2000, Vol. 31, Issue 12, pp. 1373–1381.
- 13 8. S. Geinitz, M. Eberhardt, D. Walser, D. Grund, B. Hollaus, A. Wedel, Simultaneous multi-frequency dielectric measurement  
14 technique for fast curing reactions, in *NDT.net (Hg.) 2018 – 10th International Symposium on NDT* 2019, Vol. 13.
- 15 9. A. H. Tan, K. R. Godfrey, The generation of binary and near-binary pseudorandom signals: an overview. *IEEE Trans. In-*  
16 *strum. Meas. (IEEE Transactions on Instrumentation and Measurement)* 2002, Vol. 51, Issue 4, pp. 583–588.
- 17 10. A. van den Bos, R. G. Krol, Synthesis of discrete-interval binary signals with specified Fourier amplitude spectra. *Internat-*  
18 *ional Journal of Control* 1979, Vol. 30, Issue 5, pp. 871–884.
- 19 11. M. Min, R. Land, T. Paavle, T. Parve, P. Annus, D. Trebbels, Broadband spectroscopy of dynamic impedances with short  
20 chirp pulses. *Physiological measurement* 2011, Vol. 32, Issue 7, pp. 945–958.
- 21 12. B. Sanchez, G. Vandersteen, R. Bragos, J. Schoukens, Optimal multisine excitation design for broadband electrical imped-
- 22 *ance spectroscopy. Meas. Sci. Technol. (Measurement Science and Technology)* 2011, Vol. 22, Issue 11, 115601.
- 23 13. B. Sanchez, G. Vandersteen, R. Bragos, J. Schoukens, Basics of broadband impedance spectroscopy measurements using  
24 periodic excitations. *Meas. Sci. Technol. (Measurement Science and Technology)* 2012, Vol. 23, Issue 10, 105501.
- 25 14. M. Schroeder, Synthesis of low-peak-factor signals and binary sequences with low autocorrelation. *IEEE Transactions on*  
26 *Information Theory* 1970, Vol. 16, Issue 1, pp. 85 – 89.
- 27 15. D. J. Newman, An L1 extremal problem for polynomials. *Proc. Am. Math* 1965, Vol. 16, pp. 1287–1290.
- 28 16. J. Ojarand, M. Min, Recent Advances in Crest Factor Minimization of Multisine. *EIAEE (Elektronika ir Elektrotechnika)*  
29 2017, Vol. 23, Issue 2, pp. 59–62.
- 30 17. J. Ojarand, M. Min, P. Annus, Crest factor optimization of the multisine waveform for bioimpedance spectroscopy. *Physi-*  
31 *ological measurement* 2014, Vol. 35, Issue 6, pp. 1019–1033.
- 32 18. P. J. M. van Laarhoven, E. H. L. Aarts, *Simulated Annealing: Theory and Applications*, Springer Netherlands, Dordrecht  
33 1987.
- 34 19. A. E. Eiben, J. E. Smith, *Introduction to Evolutionary Computing*, Springer Berlin Heidelberg, Berlin, Heidelberg 2015.